ABCG1 regulates mouse adipose tissue macrophage cholesterol levels and ratio of M1 to M2 cells in obesity and caloric restriction[S]

Hao Wei,[*,†] Elizabeth J. Tarling,[§,] Timothy S. McMillen,[*,†] Chongren Tang,[*,†] and Renée C. LeBoeuf[1,*,†]**

Division of Metabolism, Endocrinology and Nutrition, Department of Medicine,* and Diabetes and Obesity Center of Excellence,† University of Washington, Seattle, WA 98109-8050; and Department of Medicine§ and Department of Biological Chemistry,** David Geffen School of Medicine at University of California, Los Angeles, Los Angeles, CA 90095-1737

Abstract In addition to triacylglycerols, adipocytes contain a large reserve of unesterified cholesterol. During adipocyte lipolysis and cell death seen during severe obesity and weight loss, free fatty acids and cholesterol become available for uptake and processing by adipose tissue macrophages (ATMs). We hypothesize that ATMs become cholesterol enriched and participate in cholesterol clearance from adipose tissue. We previously showed that ABCG1 is robustly upregulated in ATMs taken from obese mice and further enhanced by caloric restriction. Here, we found that ATMs taken from obese and calorie-restricted mice derived from transplantation of WT or Abcg1-deficient bone marrow are cholesterol enriched. ABCG1 levels regulate the ratio of classically activated (M1) to alternatively activated (M2) ATMs and their cellular cholesterol content. Using WT and Abcg1$^{-/-}$ cultured macrophages, we found that *Abcg1* is most highly expressed by M2 macrophages and that ABCG1 deficiency is sufficient to retard macrophage chemotaxis. However, changes in myeloid expression of *Abcg1* did not protect mice from obesity or impaired glucose homeostasis.[JLR] Overall, ABCG1 modulates ATM cholesterol content in obesity and weight loss regimes leading to an alteration in M1 to M2 ratio that we suggest is due to the extent of macrophage egress from adipose tissue.—Wei, H., E. J. Tarling, T. S. McMillen, C. Tang, and R. C. LeBoeuf. **ABCG1 regulates mouse adipose tissue macrophage cholesterol levels and ratio of M1 to M2 cells in obesity and caloric restriction.** ***J. Lipid Res.*** **2015.** 56: **2337–2347.**

Supplementary key words mice • ATP binding cassette transporter A1 • ATP binding cassette transporter G1 • diabetes • fatty acid • gallstones • acyl-CoA:cholesterol acyltransferase • lipids • nutrition • sterols

Obesity remains highly prevalent in this country and is an important health issue because it poses an increased risk for several metabolic diseases including cancer and cardiovascular, liver, and gallbladder diseases (1–5). Obesity is accompanied by increased inflammation as evidenced systemically by elevations in circulating inflammatory cytokines and in adipose tissue due to the accumulation of adipose tissue macrophages (ATMs) (6, 7). ATMs are broadly characterized as classically activated (M1), producing proinflammatory proteins, and alternatively activated (M2) macrophages based on their responses to specific T helper (Th) 1 and Th2 cytokines (8–10). M2 ATMs are the prevalent type in lean adipose tissue, but quantitative increases in both M1 and M2 ATMs are seen with obesity (11, 12). Increases in the number of M1 macrophages and the ratio of M1 to M2 ATMs have been positively correlated to insulin resistance in humans and mice (11, 13). Thus, identifying proteins able to alter adipose tissue inflammation may aid in reducing aberrant glucose metabolism and improving obesity.

In obese humans and mice, the distribution of ATMs occurs frequently in clusters adjacent to or surrounding lipid droplets of perilipin-negative adipocytes suggesting that ATMs participate in eliminating dead fat cells (14–16). Clusters of ATMs are also seen during acute caloric restriction in mice (17). These ATMs have the appearance of foam cells similar to what is seen in atherosclerotic plaques and have been shown to contain neutral lipids based on histochemical stains (16). However, the chemical composition of these neutral lipids has not been carefully analyzed

This work was supported by National Institutes of Health Grant HL055362 (R.C.L. and C.T.), National Institutes of Health National Heart, Lung, and Blood Institute Grant HL118161 (E.J.T.), American Heart Association Western States Affiliate Postdoctoral Fellowship 11POST7300060 (E.J.T.), and Beginning Grant in Aid 13BGIA17080038 (E.J.T.). The contents are solely the responsibility of the authors and do not necessarily represent the views of the National Institutes of Health or American Heart Association. Disclosures: None relevant to this study.

Manuscript received 31 August 2015 and in revised form 7 October 2015.

Published, JLR Papers in Press, October 21, 2015
DOI 10.1194/jlr.M063354

Abbreviations: ac-LDL, acetylated LDL; ATM, adipose tissue macrophage; BMDM, bone marrow derived macrophages; BMT, bone marrow transplantation; *db/db*, C57BLKS-Lepr$^{db/J}$; DPBS, Dulbecco's PBS; FACS, fluorescence-activated cell sorting; HFD, high-fat diet; IL, interleukin; IPGTT, intraperitoneal glucose tolerance test; LXR, liver X receptor; M1, classically activated; M2, alternatively activated; MCP1, monocyte chemoattractant protein 1; SVF, stromal vascular fraction.

[1]To whom correspondence should be addressed.
e-mail: leboeuf@u.washington.edu

[S] The online version of this article (available at http://www.jlr.org) contains a supplement.

to our knowledge. Further, direct measures of ATM sterol content and in particular cholesterol have not been determined.

In humans, adipose tissue contains the largest pool of free cholesterol in the body, estimated at 25% of total body cholesterol (18–20) (1.6 mg/g adipose lipid), and this can double in obese individuals (21). Storage of free cholesterol increases markedly in hypercholesterolemic humans (22) and animals (23) providing a buffer for whole body cholesterol storage (19). Free cholesterol serves to maintain the monolayer surrounding the triacylglycerol lipid droplet and to support the structure and function of the plasma membrane (24, 25). Adipocyte lipolysis is elevated in obesity and particularly during demand lipolysis that occurs during dieting commonly used for reduction in body weight (17, 26). In addition, adipocyte death is increased in obesity and during acute weight loss. Together, these events generate large quantities of free cholesterol that must be cleared from adipose tissue.

Adipocytes can conduct cholesterol efflux as mediated by ABCA1 and scavenger receptor class B type I to lipid acceptors such as HDLs (27–29). However, these pathways may be severely reduced with adipose tissue inflammation as seen in obesity and during acute caloric restriction (29). Thus, mechanisms whereby the bulk of adipose tissue cholesterol is removed from adipose tissue in obesity and during weight loss regimes remain unclear.

We suggest that an important process for removal of free cholesterol from adipose tissue involves the cholesterol loading of ATMs from adipocytes via collision-based diffusion and/or pinocytosis of dead adipocytes. This would then be followed by cholesterol efflux from macrophages to cholesterol acceptors within adipose tissue and/or by macrophage egress from adipose tissue. Here, we show for the first time that ATMs taken from obese mice and mice undergoing acute body weight loss are enriched in cholesterol, supporting our hypothesis that ATMs participate in adipose tissue cholesterol modulation.

We previously found that the expression of *Abcg1* is markedly elevated in ATMs isolated from obese mice and that expression is further enhanced following caloric restriction (17). These data are in line with the finding that *ABCG1* is one of the most upregulated genes in human adipose tissue samples after weight loss (30). ABCG1 is a member of the ABC superfamily of transmembrane transporters that facilitate the transport of diverse substrates across membranes (31, 32). ABCG1 coordinates the intracellular distribution of cholesterol and other sterols and promotes cellular cholesterol efflux to a variety of lipid acceptors including HDL, LDL, and other phospholipid-enriched particles (32, 33). *Abcg1* expression is induced following activation of the nuclear receptor liver X receptor (LXR) by either synthetic or endogenous ligands that include specific oxysterols and desmosterol (34). Thus, *Abcg1* expression is induced following sterol loading of various cell types including endothelial cells (35), macrophages (36), atherosclerotic foam cells (37), and peritoneal macrophages taken from obese mice (17). Here, we test the possibility that *Abcg1* is a marker for cholesterol-enriched ATMs and that *Abcg1* plays a key role in modulating ATM cholesterol levels in obesity and acute weight loss.

ATMs were collected from mice for which the myeloid cells had been replaced by bone marrow transplantation (BMT) from $Abcg1^{-/-}$ mice and from WT mice undergoing autologous BMT. We found that *Abcg1* expression affected the steady-state cholesterol levels of ATMs, with $Abcg1^{-/-}$ ATMs having the highest total cholesterol content. Other sterol species were not evaluated due to limitations in ATM cell quantities. We found that the ratio of M1 to M2 ATMs was altered with loss of *Abcg1* expression, and that *Abcg1* was most highly expressed by M2 rather than proinflammatory M1 macrophages suggesting that M2 cells have a unique role in adipose tissue sterol homeostasis.

Overall, this study identifies ABCG1 as an important protein determining the relative levels of ATMs and cholesterol metabolism especially in M2 macrophages. Understanding the contribution of ABCG1 to ATM cholesterol homeostasis may provide new information for controlling obesity, weight loss, and related disorders such as lung, liver, and gallbladder diseases (38–40).

MATERIALS AND METHODS

Mice

Isogenic WT C57BL/6 mice were purchased from the Jackson Laboratory (Bar Harbor, ME; #000664). ABCG1 knockout ($Abcg1^{-/-}$) mice on a C57BL/6 background were generated as previously described (41). BMT was conducted using C57BL/6 male mice as acceptors of either C57BL/6 bone marrow cells (WT-BMT) or cells from $Abcg1^{-/-}$ mice ($Abcg1^{-/-}$ BMT) using procedures as described below. Femurs taken from $Abcg1^{-/-}$ mice were placed in PBS and sent overnight on ice from the University of California, Los Angeles to the University of Washington where bone marrow cells were isolated. In addition, C57BL/6 male mice raised at the University of Washington (three to four generations from the Jackson Laboratory) were used as a reference strain for measures of body composition. All mice were housed in pathogen-free conditions, in a temperature- and humidity-controlled environment (12 h light/dark cycle). Animal procedures were reviewed and approved by the Institutional Animal Care and Use Committee of University of Washington.

Study design

BMT was performed essentially as described (42). Briefly, male C57BL/6 mice (WT) at 13 weeks of age were irradiated (950 rads) and then engrafted with either WT or $Abcg1^{-/-}$ bone marrow cells (5×10^6 cells/mouse; n = 20 in each group) by retro-orbital injection. Mice were maintained on pelleted rodent chow (LabDiet 5053; Purina Mills, St. Louis, MO) and acidified water with neomycin (X-gen Pharmaceuticals, Big Flats, NY) for 4 weeks of recovery. Mice were then fed a high-fat diet (HFD) [D12492; Research Diets Inc., New Brunswick, NJ; 60% kcal (primarily lard) and 20% kcal carbohydrate (maltodextrin 10 and sucrose)] for 13 weeks. Mice were then randomly assigned to one of two groups for another 3 weeks of either continued ad libitum HFD feeding or to caloric restriction. For caloric restriction, mice were individually housed and given 60% of the HFD food consumption as monitored during weeks 10–12 as described (43). At the end of all feeding studies, mice were fasted for 4 h in the morning, bled from the retro-orbital sinus into tubes containing 1 mM

EDTA to obtain plasma, and euthanized by cervical dislocation, and tissues were collected for analyses. An aliquot of epididymal fat was immediately used to isolate ATMs (see below).

Body composition and glucose tolerance

In vivo body composition analysis of lean and fat mass content was performed before and 2 weeks after caloric restriction using quantitative magnetic resonance (EchoMRI™ 3-in-1 Animal Tissue Composition Analyzer; Echo Medical Systems, Houston, TX) (44, 45). Intraperitoneal glucose tolerance tests (IPGTTs) were conducted as described (43, 46).

Stromal vascular fraction isolation and fluorescence-activated cell sorting

Epididymal fat pads were excised and minced in Dulbecco's PBS (DPBS with calcium chloride and magnesium; Life Technologies, Grand Island, NY). Tissue suspensions were centrifuged (500 *g*, 5 min) followed by incubation with 1 mg/ml collagenase (Sigma-Aldrich, St. Louis, MO) at 37°C for 20 min with shaking. The cell suspension was filtered through a 100 μm filter and then centrifuged (300 *g*, 5 min) to separate adipocytes from the stromal vascular fraction (SVF) pellet. For fluorescence-activated cell sorting (FACS), the SVF pellet was resuspended and incubated in 0.5 ml RBC Lysis Buffer (eBioscience, San Diego, CA) for 5 min. The SVF was washed and pelleted in DPBS and then resuspended in sorting buffer (eBioscience). Cells were incubated with Fc Block (eBioscience) prior to staining with conjugated antibodies or isotype controls for 15 min at 4°C followed by two washes in 10× DPBS. Cells were resuspended in DPBS supplemented with propidium iodide to assess cell viability and then subjected to FACS (FACSAria; BD Biosciences, San Jose, CA). Viable cells were sorted directly into DPBS, pelleted, and frozen at −80°C for further analysis. Antibodies used in FACS were as follows: F4/80-FITC, CD11c-PerCP5.5, CD45-eFluor450 (eBioscience), and CD206-PECy7 (AbD Serotec; Bio-Rad Laboratories Inc., Hercules, CA).

Quantification of cellular cholesterol

Cells were resuspended in 100 μl DPBS, and cholesterol-d7 (Sigma-Aldrich) was added as the internal standard. After saponification, the lipid fraction was extracted from the membrane preparation with hexane and dried under nitrogen gas. Total cholesterol levels were determined after derivatization using LC/MS/MS as described (47). Unesterified cholesterol was measured using the same procedure except without the saponification step, and the quantity of cholesterol moiety of cholesteryl ester was calculated indirectly using the following equation: cholesterol moiety of cholesteryl ester = total cholesterol − unesterified cholesterol.

Bone marrow-derived macrophage differentiation

Bone marrow cells isolated from femurs of 10-week-old WT and *Abcg1*$^{-/-}$ mice were cultured in low-glucose DMEM (Thermo Scientific, Rockford, IL) supplemented with 10% FBS (Life Technologies), macrophage-colony stimulating factor [30% L-929-conditioned medium prepared as described (48)] for differentiation into macrophages. By day 7, macrophages were polarized with 5 ng/ml lipopolysaccharide and 12 ng/ml IFNγ (M1) or 10 ng/ml interleukin (IL) 4 (M2). Nonpolarized macrophages [bone marrow-derived macrophages (BMDMs)] were cultured in complete medium alone. At days 9 and 10, cells are used for mRNA extractions or chemotaxis assays.

Chemotaxis assay

Macrophage migration was determined as described (49). Briefly, macrophages were incubated with 1 μg/ml Calcein AM (Invitrogen) for 30 min at 37°C. Cells were then washed with DPBS and resuspended in RPMI 1640 medium with 0.1% free fatty acid-free BSA (Sigma-Aldrich) to a final concentration of 1×10^6 cells/ml. Cell migration was assessed using the disposable 96-well ChemoTx System 101-3 (Neuro probe, Gaithersburg, MD) according to the manufacturer's instructions. Recombinant monocyte chemoattractant protein 1 (MCP-1) (Biolegend, San Diego, CA) at 50 ng/μl was used as chemoattractant to trigger cell migration. The fluorescence of cells was measured using Synergy4 microplate reader (Bio-Tek, Winooski, VT). Percentages of cell migration were calculated as migrated cells/loading control (cells loaded directly to the bottom of the well), corrected for spontaneous migration. Each sample was tested in 6 wells.

Cholesterol loading of macrophages

Macrophages were suspended in DMEM medium containing 1 mg/ml BSA and 100 μg/ml acetylated LDL (ac-LDL) and incubated for 24 h prior to cell collection and usage for mRNA or migration studies.

Immunoblotting

Mouse cells were homogenized in lysis buffer (0.1 M K_2HPO_4, 1 mM PMSF, 0.2% Triton X-100, and 0.1% protease inhibitor cocktail; P8340, Sigma). The homogenate was centrifuged (12,000 *g* for 10 min at 4°C), and the supernatant was collected. Equal amounts of protein (20 μg) were electrophoresed on 15% SDS polyacrylamide gels and then electro-transferred to a ProTran nitrocellulose membrane (Schleicher and Schuell, Riviera Beach, FL). Protein levels were measured by immunoblots using antibodies for ABCA1 (Novus Biological, Littleton, CO), ABCG1 (Cell Signaling Technology, Danvers, MA), and GAPDH (Abcam, Boston, MA), and then probed with horseradish peroxidase secondary antibody (Chemicon International, Temecula, CA). Blots were developed using SuperSignal pico ECL kit (Pierce, Thermo Scientific, Waltham, MA). Molecular band intensity was determined by densitometry using National Institutes of Health ImageJ software.

Real-time quantitative RT-PCR

Total RNA was extracted from adipose tissue or cells using TRIzol Reagent (Invitrogen, Carlsbad, CA). cDNA was synthesized using Superscript III reverse transcriptase (Epicentre Biotechnologies, Madison, WI) and random hexamer primers. mRNA levels of mouse Nos2 (nitric oxide synthase 2) (50), Chil3 (chitinase-like 3), Il6, Arg1 (arginase), Abca1, Abcg1, Acat, MCP1, and L32 were measured by real-time RT-PCR using the 7500 real-time PCR System (Applied Biosystems, Foster City, CA) and SybrGreen Master Mix (Bioline USA Inc., Tauton, MA). PCR reactions were performed in duplicate, and the data were analyzed with the ddCt method as previously described (51). After normalization to internal control L32, the results for each target gene were expressed as fold change from WT control. Primer sequences are listed in supplementary Table 1.

Statistical analysis

All results are reported as mean ± SEM and analyzed using unpaired Student's *t*-test following log10 transformation of data and nonparametric ANOVA (Bonferroni correction) followed by multiple comparisons as appropriate. Differences are considered statistically significant at the $P < 0.05$ level.

RESULTS

ATM cholesterol content is enriched by obesity and further enhanced following caloric restriction

We tested the hypothesis that ATMs become cholesterol enriched due to obesity and following body fat loss induced by caloric restriction. FACS was used to isolate

F4/80$^+$ ATMs from epididymal adipose tissues taken from mice, and LC/MS/MS was used to quantify cholesterol levels. Oxysterol quantities were not evaluated at this time due to the small numbers of available cells. We were also unable to detect cholesterol in ATMs taken from lean mice due to low cell numbers and likely low levels of total cholesterol.

Obese mice and mice subjected to caloric restriction were from two studies. First, we used tissues taken from genetically obese *db/db* (C57BLKS-Lepr$^{db/J}$) mice studied previously (17). These mice are of the C57BLKS background, and their diets and handling are described (17). The body fat content for *db/db* mice was markedly higher than seen for C57BLKS lean controls and was reduced by nearly 50% following caloric restriction (17). Second, diet-induced obesity and caloric restriction were applied to WT C57BL/6 mice as described herein, and tissues were taken for analysis. This was a separate set of WT mice than those used with the BMT study. Body fat content was reduced significantly following caloric restriction (supplementary Table 2).

As compared with lean counterparts for which total cholesterol levels could not be detected, total cholesterol levels for F4/80$^+$ ATMs from *db/db* obese and diet-induced WT obese mice (**Fig. 1A**) were near 1.0 pg/cell. Following caloric restriction, total cholesterol levels were significantly elevated to >2.0 pg/cell.

For *db/db* mice, we were able to isolate broad subsets of F4/80$^+$ cells into M1 (CD11c$^+$CD206$^-$) and M2 (CD11c$^-$CD206$^+$) ATMs using FACS (11, 12) and then quantify total cholesterol in each cell population. We found that for ad libitum fed obese mice, significantly more total cholesterol was seen within M2 cells than M1 ATMs (Fig. 1B). For both subpopulations, total cholesterol levels were significantly increased following caloric restriction with the higher levels of cholesterol seen in M2 cells (Fig. 1B). These data suggest that M2 cells play a particularly important role in adipose tissue remodeling and cholesterol homeostasis.

Overall, although macrophage cholesterol synthesis cannot be discounted, ATM cholesterol enrichment is most likely due to uptake of adipocyte-derived cholesterol because cholesterol would be readily available as a result of high rates of adipocyte lipolysis and cell death as seen in obesity and caloric restriction.

Abcg1 genotype determines cholesterol content of ATMs in obese mice

Abcg1 is highly expressed in ATMs of obese mice (17) and adipose tissue in humans (30). To determine whether ATM cholesterol levels are controlled in part by ABCG1, we compared cellular cholesterol levels and chemical composition between WT-BMT and *Abcg1*$^{-/-}$ BMT mice.

ATM cholesterol levels were significantly higher for *Abcg1*$^{-/-}$ BMT than WT-BMT mice in both obese and caloric-restricted states (**Fig. 2A**). More than 90% of total cholesterol was unesterified (Fig. 2B). We found that the levels of unesterified cholesterol significantly increased with caloric restriction for WT-BMT mouse ATMs but did not change for *Abcg1*$^{-/-}$ BMT mice (Fig. 2B). Interestingly, following caloric restriction, the ATM population isolated from *Abcg1*$^{-/-}$ BMT mice showed a marked elevation in cholesteryl ester content as compared with ATMs taken from WT-BMT tissues, signifying a greater storage of cholesterol in intracellular lipid droplets for *Abcg1*-deficient cells (Fig. 2C). In support of this latter finding is the significantly elevated expression of *Acat* found for calorically restricted *Abcg1*$^{-/-}$ BMT mouse adipose tissue (**Fig. 3A**).

These data are the first report that *Abcg1* deficiency influences ATM cholesterol content and are consistent with the role of *Abcg1* to mobilize and efflux cellular cholesterol as seen by others (41, 52, 53). Overall, ABCG1 is needed in adipose tissue to reduce intracellular cholesterol levels of ATMs in obesity and during caloric restriction.

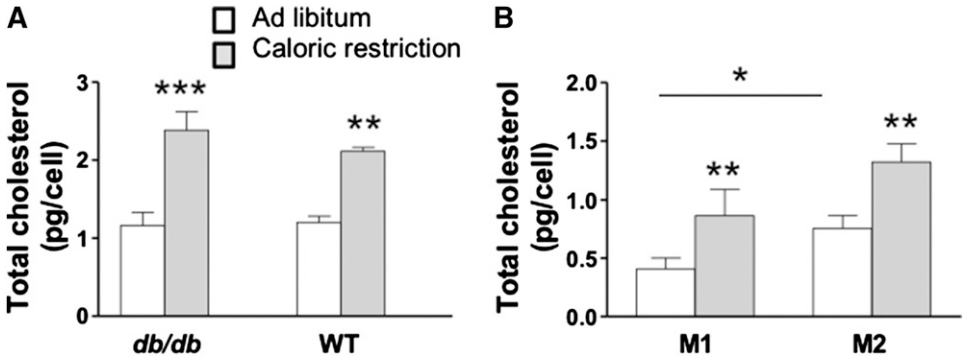

Fig. 1. Total cholesterol levels in ATMs taken from obese mice. Epididymal adipose tissue was collected from mice fed ad libitum (open bar) or subjected to caloric restriction (gray bar) (A). The *db/db* mice were fed rodent chow and treated as described previously (17). WT mice were fed the HFD and their treatment is described in Materials and Methods. ATMs from *db/db* mice were further categorized based on their surface expression of CD11C and CD206 to assess the subpopulation of M1 (CD11C$^+$CD206$^-$) and M2 (CD11C$^-$CD206$^+$) and isolated by FACS (B). Total cholesterol levels were quantified using LC/MS/MS. Data are presented as mean ± SEM. * $P < 0.02$; ** $P < 0.001$; *** $P < 0.0004$ for n = 10–11 mice per strain and n = 6 ATM samples.

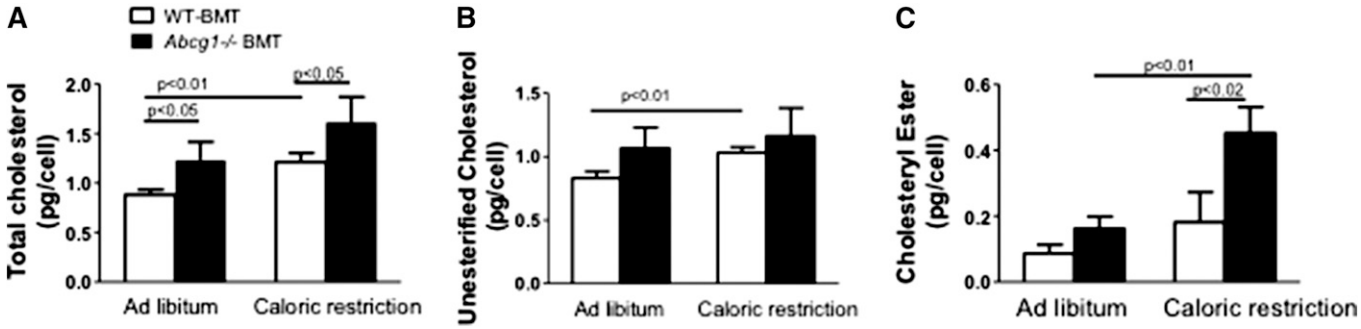

Fig. 2. Deficiency in myeloid cell ABCG1 modulates ATM cholesterol levels. WT male C57BL/6 mice were irradiated and then two separate groups were engrafted with bone marrow from either WT (WT-BMT) (open bars) or *Abcg1*$^{-/-}$ (*Abcg1*$^{-/-}$ BMT) mice (black bars) (A–C). Animals were fed an HFD for 13 weeks and then subjected to 3 weeks of caloric restriction or maintained ad libitum on the HFD. ATMs were collected using FACS as described in Materials and Methods. Total (A), unesterified (B), and esterified (C) cholesterol levels were quantified using LC/MS/MS. Values are presented as mean ± SEM (n = 5), and *P* values are shown in the figure.

Abcg1 genotype modulates M2 content in adipose tissue

Several tissues of *Abcg1*$^{-/-}$ mice, including lungs and aorta, have been shown to accumulate lipids and exhibit inflammation (41, 54–56). Because ATMs accumulated cholesterol in the *Abcg1*$^{-/-}$ BMT ATMs as compared with WT-BMT cells, we tested whether inflammation was also elevated in adipose tissue of *Abcg1*-deficient mice. Total ATMs (F4/80^{+}) and M1 (CD11c^{+}CD206^{-}) and M2 (CD11c^{-}CD206^{+}) ATMs were isolated by FACS, and then cell counts were compared between mouse strains.

With caloric restriction, inflammation was decreased significantly for WT-BMT but not for *Abcg1*$^{-/-}$ BMT mice as evidenced by significant decreases in the total number of ATMs (F4/80^{+}) (**Fig. 4A**) and M1 cells for WT-BMT mice (Fig. 4B). In addition, tissue levels of MCP-1 and Il6, molecular markers associated with inflammation, were significantly reduced in adipose tissue samples of WT-BMT but not *Abcg1*$^{-/-}$ BMT mice following caloric restriction (Fig. 3B, C). A major finding was the marked and significant increase (>2-fold) in numbers of M2 macrophages found for *Abcg1*$^{-/-}$ BMT mice as compared with their WT-BMT controls (Fig. 4C). This was associated with a significant decrease in M1 to M2 ratio for ad libitum fed *Abcg1*$^{-/-}$ BMT mice as compared with WT-BMT controls (Fig. 4D). These data show that the loss of *Abcg1* influences the extent of adipose tissue inflammation and leads to an increase in M2 macrophages. We suggest that differences in the immune status between WT-BMT and *Abcg1*$^{-/-}$ BMT mice are related to their ATM cholesterol contents.

Abcg1 deficiency results in impaired macrophage migration

The absence of inflammatory reduction by caloric restriction and higher M2 ATM levels seen for *Abcg1*$^{-/-}$ BMT mice as compared with WT-BMT mice (Fig. 4C) may be due in part to decreased egress of ATMs from adipose tissue. In support of this concept for ATMs, Pagler et al. (57) demonstrated that cholesterol loading of peritoneal macrophages taken from double-deficient *Abca1*$^{-/-}$*Abcg1*$^{-/-}$ mice displayed impaired chemotaxis that was due to defects in Rac1/Rho GTPase activities that were in turn due to an alteration in plasma membrane cholesterol distribution. Here, we test the hypothesis that loss of *Abcg1* expression is sufficient to reduce ATM chemotaxis.

To test this hypothesis, M1 and M2 macrophages were differentiated from WT and *Abcg1*$^{-/-}$ bone marrow cells, and their migration capability was evaluated using a microplate chemotaxis system toward MCP1 in the absence and presence of cholesterol loading. MCP1 is a convenient and powerful monocyte attractant, and levels of expression were markedly reduced in WT-BMT following caloric restriction in concert with reduced tissue inflammation in

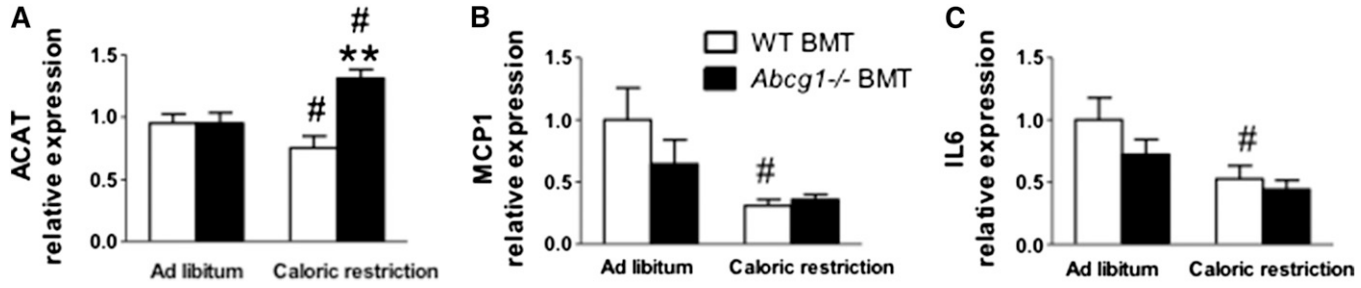

Fig. 3. mRNA levels for cholesterol metabolism and inflammatory genes in epididymal tissues taken from mice. WT-BMT (open bars) and Abcg1$^{-/-}$ BMT (black bars) were treated as described in Figure 2. mRNA was isolated and PCR performed as described in Materials and Methods. mRNA results are expressed as fold induction as compared with WT-BMT (WT-BMT = 1 arbitrary unit). Values are presented for ACAT (A), MCP1 (B), and IL-6 (C). Data are expressed as mean ± SEM for n = 8 mice. ** $P < 0.03$ between WT-BMT and *Abcg1*$^{-/-}$ BMT. # $P < 0.003$ between ad libitum and caloric restriction treatments within the same mouse strain.

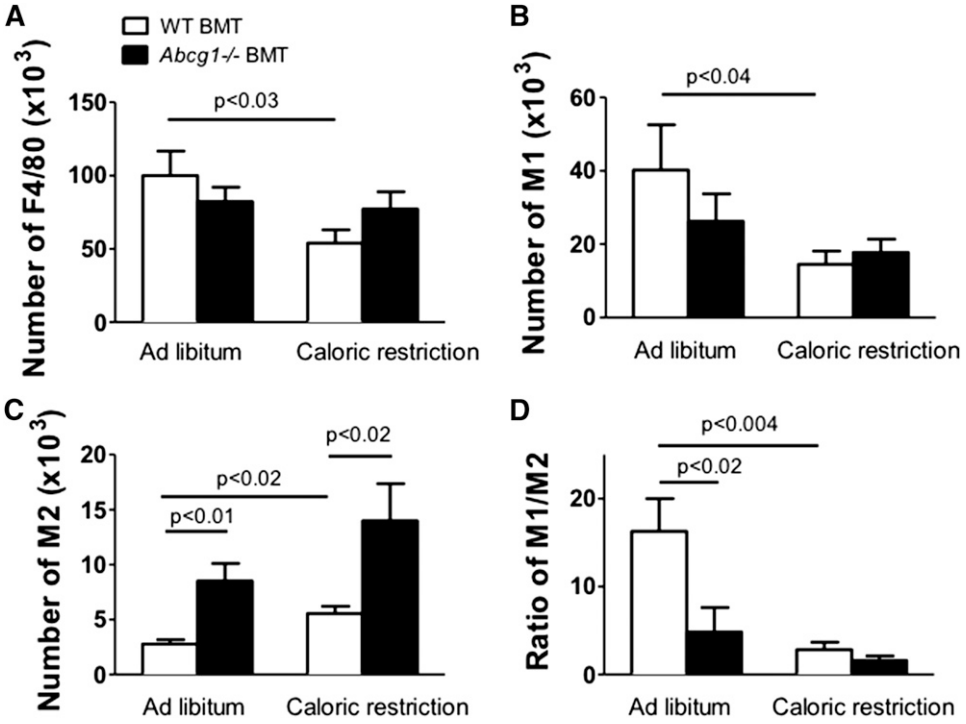

Fig. 4. Loss of *Abcg1* expression increases the numbers of M2 but not M1 ATMs. WT-BMT and Abcg1$^{-/-}$ BMT were generated and treated as described in Figure 2. ATMs were collected using FACS as described in Materials and Methods. Values are given for numbers of total F4/80^{+} cells (A), M1 ATMs (B), M2 ATMs (C), and the ratio of M1 to M2 cells (D) for mice in ad libitum and caloric restriction groups. Data are presented as mean ± SEM (n = 4–5). *P* values are show in the figure.

these mice. Confirmation of appropriate differentiation was seen using gene markers associated with M1 and M2 macrophages (supplementary Fig. 1A, B) (11, 58). As expected, *Nos2* and *Il6* were highly expressed by M1 cells, and *Chil3* and *Arg1* were markedly elevated in M2 cells. Importantly, differentiation of these cells was not aberrant for *Abcg1*$^{-/-}$ mice (supplementary Fig. 1B).

In the absence of cholesterol loading, *Abcg1*$^{-/-}$ M2 but not M1 cells exhibited impaired chemotaxis (~40%) as compared with WT cells (**Fig. 5**). This finding points to an important role for ABCG1 in M2 basal sterol homeostasis. After cholesterol loading with ac-LDL, M1 and M2 cells from *Abcg1*$^{-/-}$ mice exhibited reduced migration capacity. In addition, M2 cells from WT mice also show significant reduction in chemotaxis as compared with their basal state. These data demonstrate for the first time that loss of *Abcg1* alone is sufficient to impair cytokine migration functions in macrophages. In addition, these data show that M2 cells in general are particularly sensitive to cholesterol homeostasis with respect to chemotactic functions.

We suggest that the absence of inflammatory reduction following caloric restriction and the higher M2 ATM levels that are seen for *Abcg1*$^{-/-}$ BMT mice as compared with WT-BMT mice (Fig. 4C) are due in part to decreased egress of *Abcg1*$^{-/-}$ ATMs from adipose tissue.

Abcg1 is preferentially expressed by M2 macrophages

We next tested the hypothesis that *Abcg1* expression and thereby mechanisms of cellular sterol balance may differ between M1 and M2 macrophages. BMDMs were taken from WT mice and differentiated in culture into M1 and M2 macrophages using standard cytokine inductions. Confirmation of appropriate differentiation was seen using gene markers associated with M1 and M2 macrophages (supplementary Fig. 1) (11, 58). *Abcg1* mRNA and protein levels were then quantified (**Fig. 6A–**C) and compared with another protein known to modulate cholesterol efflux, *Abca1* (Fig. 6D–F).

The expression of *Abcg1* and *Abca1* were examined under basal and cholesterol-loaded conditions to recapitulate what might be experienced by macrophages under lean and obese body weight statuses, respectively. Under basal conditions, M2 cells expressed substantially higher *Abcg1* mRNA (5-fold) than BMDM or M1 macrophages (Fig. 6A). This was substantiated at the level of protein by immunoblotting (Fig. 6B, C). In contrast, the expression of *Abca1* was comparable across cell types with respect to mRNA (Fig. 6D) and protein (Fig. 6E, F). Together, these data demonstrate that M2 macrophages have specificity for *Abcg1* expression, and it is likely that *Abcg1* has important functions in this cell type.

Cholesterol loading increases the expression of *Abcg1* and *Abca1* via regulation by LXRs (34, 59, 60). After cholesterol loading, *Abcg1* expression increased for all cell types, but the highest relative expression remained with M2 cells (33%) (Fig. 6A). The expression of *Abca1* was also enhanced by cholesterol treatment, but the magnitude of change was smallest for M2 cells (Fig. 6D). For these studies, we did not have enough cells remaining for immunoblotting but believe that mRNA reflects protein levels based

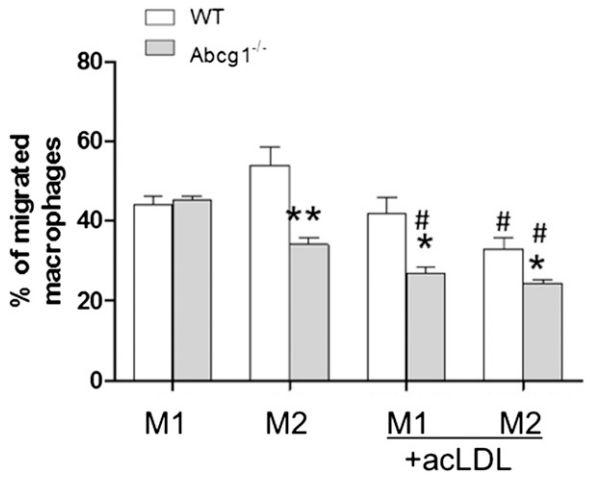

Fig. 5. Deletion of ABCG1 is sufficient to impair macrophage migration. Bone marrow cells from C57BL/6 (WT) and *Abcg1*$^{-/-}$ mice were differentiated into BMDMs and further polarized into M1 and M2 macrophages as described in Materials and Methods. The migration capability of M1 and M2 macrophages from different genotypes was assessed using a microplate chemotaxis system as described in Materials and Methods. Migration capability of cells derived from WT (white bars) and *Abcg1*$^{-/-}$ (gray bars) bone marrow cells was expressed as percentage of migrated cells to total cells. Values are presented as mean ± SEM (n = 3). * $P < 0.05$ between WT and *Abcg1*$^{-/-}$ cells; ** $P < 0.01$ between WT and *Abcg1*$^{-/-}$ cells; # $P < 0.05$ between M1 and M2 macrophages within the same genotype. In both cases, n = 3; experiments were done using three separate mice per genotype.

on increases in protein signal seen following macrophage treatment with LXR agonist GW3965 (32). Together, these data demonstrate a strong preferential expression of *Abcg1* by M2 macrophages.

A limitation to these findings is that cells in culture may not demonstrate the same expression patterns as in vivo (61). However, these data are consistent with the relative expression of *Abca1* and *Abcg1* in naive peritoneal macrophages that are noninflammatory (62, 63) isolated from obese *db/db* mice for which *Abcg1* was highly expressed (17).

Abcg1 myeloid deficiency does not modulate body weight or glucose metabolism

WT mice fed the HFD have been repeatedly shown to gain body weight and fat, accompanied by systemic and adipose tissue inflammation (11, 14, 15, 43, 46, 51, 58). What is not known is whether alterations in myeloid-derived *Abcg1*$^{-/-}$ worsen obesity or alter the course of body weight and fat loss during caloric restriction. Because cholesterol uptake by ATMs may enhance their inflammatory state (15, 17), loss of ABCG1 may worsen obesity by virtue of higher ATM cholesterol levels. However, the ratio of M1 to M2 ATMs is higher for WT mice, and because this has been associated with impaired glucose tolerance and insulin resistance (12), loss of ABCG1 could improve obesity and glucose homeostasis for mice. In addition, Buchmann et al. (64) found that the absence of whole body *Abcg1* expression resulted in leaner mice with improved glucose homeostasis. We tested the hypothesis that loss of myeloid cell expression of *Abcg1* would be sufficient to alter body weight and glucose homeostasis. Body weight, body composition, and glucose metabolism were evaluated for WT-BMT and *Abcg1*$^{-/-}$ BMT mice.

Abcg1$^{-/-}$ BMT mice exhibited no differences in body weight gain (ad libitum treatment) or loss (caloric restriction treatment) as compared with WT-BMT control mice (**Fig. 7A**). Body composition evaluated at 12 and 14 weeks showed no differences in lean and fat mass between WT-BMT and *Abcg1*$^{-/-}$ BMT mice (supplementary Table 2). We also found that glucose homeostasis outcomes as evaluated using IPGTTs were comparable between *Abcg1*$^{-/-}$ BMT and WT-BMT mice (Fig. 7B). Overall, deficiency in *Abcg1* expression in myeloid-derived cells did not influence body weight or glucose homeostasis.

DISCUSSION

We show for the first time that ATMs taken from obese and acutely dieting mice are enriched in cholesterol. This was seen in a genetic model of obesity and in diet-induced obesity of normally lean mice. The cholesterol content of ATMs was particularly increased by caloric restriction, a condition of high-demand lipolysis for which the release of fatty acids and cholesterol is expected to be abundant (14, 15, 17). Using mice and cells with loss of function of ABCG1, we showed that *Abcg1* is expressed preferentially by M2 macrophages, ATM cellular cholesterol levels are modulated by *Abcg1* expression, and loss of *Abcg1* is sufficient to impair cytokine-stimulated ATM migration. Importantly, loss of *Abcg1* expression in myeloid-derived cells modulated the number of adipose tissue M2 macrophages and the ratio of M1 to M2 ATMs. These changes did not result in significant differences in body weight or glucose homeostasis between control and *Abcg1*$^{-/-}$ BMT mice.

Identifying genes that can alter the inflammatory component of obesity is important, as increases in the number of activated M1 macrophages and the ratio of M1 to M2 ATMs have been positively correlated to insulin resistance in humans and mice (11, 13). Here, loss of *Abcg1* led to significant elevations in the number of adipose tissue M2 cells as compared with the number found in WT mice, modifying the ratio of M1 to M2 ATMs. Further, loss of *Abcg1* expression altered the functionality (migration) of M2 cells as derived in culture. Thus, ABCG1 provides a molecular tool with which to study functions special to M2 cells.

Potential functions of ABCG1 in M2 macrophages are likely to involve sterol transmembrane trafficking and intracellular cholesterol pool maintenance based on previous studies (32, 33). For instance, in pancreatic β cells, ablation of *Abcg1* results in decreased insulin secretion due to an altered subcellular cholesterol distribution (33). Ablation of *Abcg1* is associated with a reduction in the bioavailability of macrophage LPL, an enzyme requiring membrane partitioning during biosynthesis, in macrophages resulting in reduced LPL-mediated lipid accumulation (54). M2 functions have been attributed to microbial

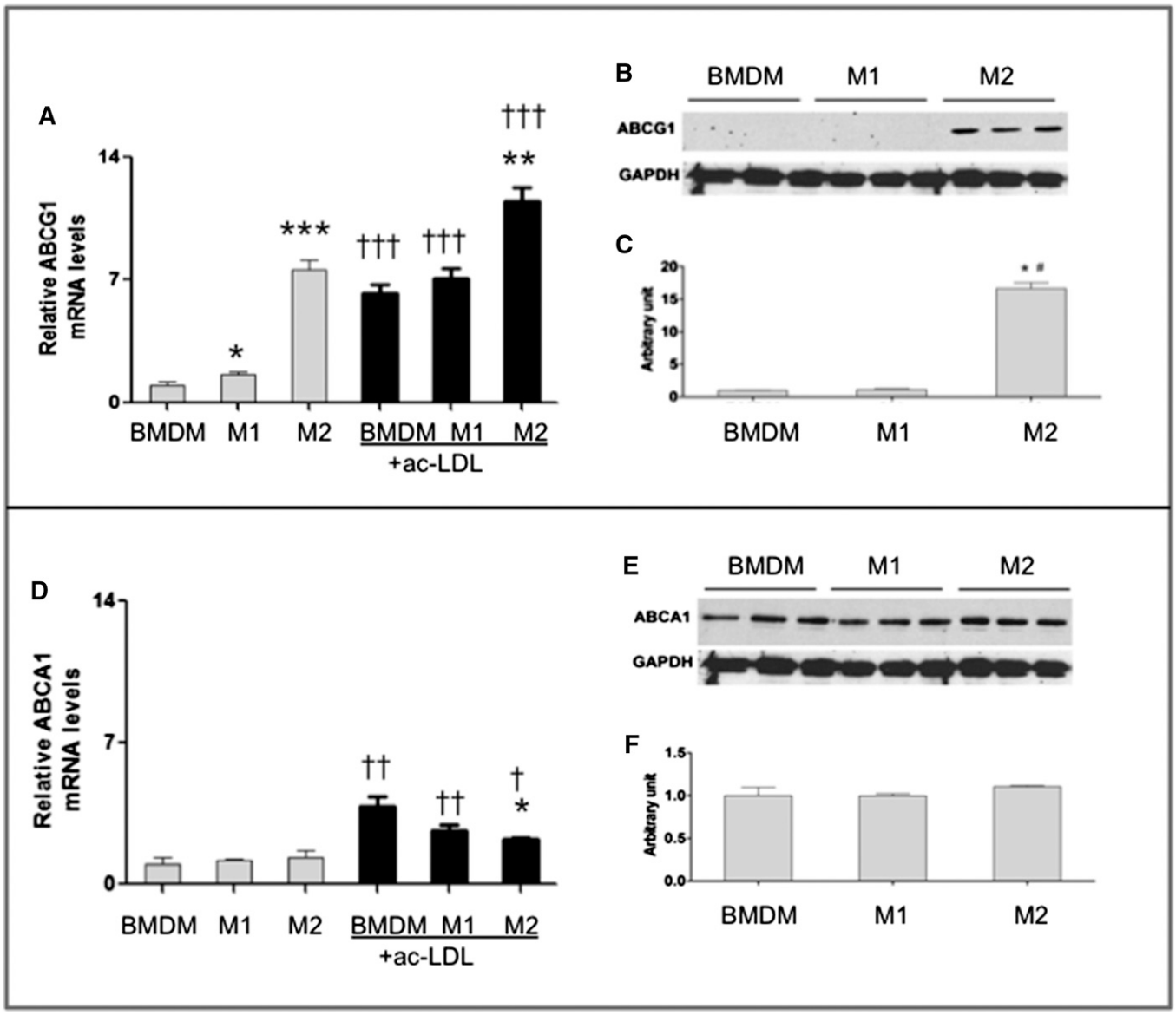

Fig. 6. *Abcg1* but not *Abca1* is preferentially expressed by M2 macrophages. BMDMs and M1 and M2 macrophages were cultured from WT (C57BL/6 male) bone marrow cells as described in Materials and Methods. mRNA and protein levels were evaluated for *Abcg1* (A–C) and *Abca1* (D–F) for cells without cholesterol loading. Additional cells were incubated with ac-LDL for 24 h and then quantified for *Abcg1* (A, black bars) and *Abca1* (D, black bars) expression. mRNA levels were quantified by RT-PCR and normalized to L32 levels. Protein was isolated from cell lysates and prepared for SDS-PAGE and immunoblotting using GAPDH as a protein loading control as in Materials and Methods. Signal bands were quantified by densitometry using National Institutes of Health ImageJ software for protein levels. Values are presented as mean ± SEM (n = 3–4). * $P < 0.05$, ** $P < 0.01$, *** $P < 0.001$ between BMDM and M1 or M2 groups within noncholesterol and cholesterol-loaded groups (n = 3); † $P < 0.05$, †† $P < 0.01$, ††† $P < 0.001$ between noncholesterol and cholesterol-loaded cells within BMDM, M1, and M2 cell types (n = 4).

monitoring, tissue repair, and tissue remodeling (65, 66), all functions likely involving lipid uptake and metabolism. Thus, ABCG1 may provide important protection for M2 macrophages with respect to the distribution and efflux of potentially chemotoxic sterols.

Evidence for specific roles for *Abcg1* in M2 cells was seen. *Abcg1* expression was elevated preferentially in M2 cells as compared with M1 cells. M2 cells derived in culture from *Abcg1*$^{-/-}$ mice showed reduced migration in the basal state as compared with cells derived from WT mice. This dramatic finding demonstrates that even without cholesterol loading, M2 cells are sensitive to functions modified by *Abcg1*.

With cholesterol loading, migration toward a cytokine stimulant was reduced in both M1 and M2 cells derived from *Abcg1*$^{-/-}$ mice. Pagler et al. (57) demonstrated that cholesterol loading of macrophages taken from double-deficient *Abca1*$^{-/-}$*Abcg1*$^{-/-}$ mice displayed impaired chemotaxis that was due to defects in Rac1/Rho activities that were in turn due to an alteration in plasma membrane cholesterol distribution. Thus, we establish for the first time that loss of *Abcg1* is sufficient to retard migration.

Impaired chemotaxis as seen for macrophages derived from *Abcg1*$^{-/-}$ mice may also explain in part differences in the extent of inflammation that was reduced by caloric

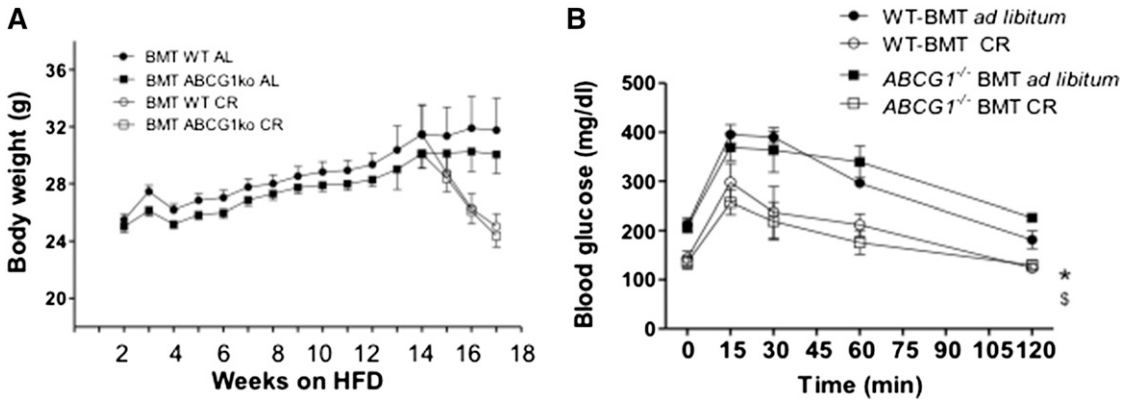

Fig. 7. Body weights and glucose status for mice that are WT or deficient in *Abcg1* expression. Animals were fed an HFD for 13 weeks and then subjected to 3 weeks of caloric restriction (CR) or maintained ad libitum on the HFD. Mouse groups are as described in Figure 2. Mice were monitored for body weight weekly. (A) No significant differences were seen between WT-BMT and *Abcg1*$^{-/-}$ BMT mice during either the ad libitum or CR arms of this study. Data are presented as means ± SEM; n = 39–40 for weeks 1–12; n = 9–10 for weeks 13–16. IPGTTs were performed at several time points as described in Materials and Methods. (B) Shown are final values for BMT mice including WT mice transplanted with WT bone marrow in the ad libitum (black circle) and CR (open circle) treatment groups, and *Abcg1*$^{-/-}$ BMT ad libitum (black square) and CR (open square) groups. Symbols shown are $P < 0.05$ between ad libitum and CR responses at 120 min. No significant differences in glucose homeostasis was seen between mouse strains within each diet treatment group for n = 5 mice per strain.

restriction in WT but not *Abcg1*$^{-/-}$ adipose tissue. Negative energy balance eventually results in loss of body fat and a reduction in local inflammation. This was evidenced in the WT mice as a reduction in numbers of total (F4/80^{+}) and M1 ATMs, as well as reduced expression of inflammatory genes MCP1 and Il6. In contrast, a dampening of inflammation was not seen for *Abcg1*$^{-/-}$ mice. In fact, the number of M2 ATMs was markedly higher for *Abcg1*$^{-/-}$ mice in both obese and negative balance states. We suggest that the increase in M2 ATMs as seen for *Abcg1*$^{-/-}$ BMT versus WT-BMT mice was due at least in part to impaired migration leading to reduced adipose tissue egress of M2 cells. This idea is based on mechanisms thought to occur in the early stages of atherosclerosis, another disorder in which macrophages accumulate cholesterol. In this case, reduced inflammation is thought to occur due to multiple pathways including an inhibition of monocyte recruitment, clearance of apoptotic cells, and/or increases in inflammatory cell egress from vascular tissue (67).

Myeloid-derived *Abcg1* deficiency was not associated with differences in body weight, body composition, or glucose status as compared with WT mice. Both strains showed significant body weight and body fat gain with feeding of the HFD accompanied by impaired glucose metabolism. These results differ from one report that whole body *Abcg1*$^{-/-}$ mice are protected from HFD-induced body weight gain (64). These mice showed improved glucose homeostasis, reduced food intake, and increased energy expenditure. Because background strain (C57BL/6), duration of diet, and dietary fat content (36% by weight) were comparable between our study and the study by Buchmann et al., these data suggest that cells other than myeloid based are critical for body weight regulation. For instance, *Abcg1* is highly expressed in brain where it contributes greatly to cholesterol homeostasis in microglia (68). Thus, a possible explanation is that ABCG1 participates in food intake and peripheral glucose homeostasis directives in the brain, a tissue for which repopulation by our bone marrow-derived cells would be poor (69). However, the findings by Buchmann et al. are somewhat in contrast to what would be expected by the finding that loss of *Abcg1* expression in pancreatic islets is associated with reduced insulin production (33). Loss of ABCG1 in these rodent chow-fed mice resulted in worsening of glucose homeostasis and reduced insulin secretion, factors recapitulating insulin resistance and obesity. Overall, the contribution of ABCG1 to states of obesity and insulin resistance are still being defined.

We studied ATM cholesterol levels and the role of ABCG1 in ATM cholesterol homeostasis in the context of obesity and caloric restriction. These are metabolic states characterized by high lipolysis rates (26), and further, acute body weight loss is associated with increased gallstone disease in humans (2, 40). It is intriguing to think that excessive release of adipose tissue cholesterol during dieting may provide a secondary source for increased hypersaturation of bile leading to gallstone formation (70). Thus, determining how cholesterol is mobilized and cleared from adipose tissue under states of high lipolysis and cell death could provide directions for prevention of metabolic complications during dieting.

In summary, novel data show that ATMs from obese mice accumulate cholesterol, the extent of which is modulated in part by levels of *Abcg1* expression. *Abcg1* is expressed primarily in M2 as opposed to M1 cells. M2 macrophages are known to participate in tissue remodeling that involves lipid clearance. Thus, it is likely that ABCG1 provides a critical role for the handling of intracellular sterols in M2 ATMs. Further studies in the role of ABCG1 in M2 macrophages will contribute to our understanding of sterol metabolism in adipose tissue in obesity as well as other diseases in which macrophages accumulate cholesterol.

The authors are grateful for the excellent insights and critical discussions of this manuscript by Dr. Peter A. Edwards (Department of Medicine and Department of Biological Chemistry, David Geffen School of Medicine at University of California Los Angeles, CA). The authors thank Dr. Cheryl Wellington (Department of Pathology and Laboratory Medicine, Centre for Brain Health, University of British Columbia, Vancouver, BC, Canada) for her kind gift of mice and helpful discussions, and Barbara Houston for her excellent husbandry and necropsy of all mice.

REFERENCES

1. Azagury, D. E., and D. B. Lautz. 2011. Obesity overview: epidemiology, health and financial impact, and guidelines for qualification for surgical therapy. *Gastrointest. Endosc. Clin. N. Am.* **21:** 189–201.
2. Banim, P. J., R. N. Luben, H. Bulluck, S. J. Sharp, N. J. Wareham, K. T. Khaw, and A. R. Hart. 2011. The aetiology of symptomatic gallstones quantification of the effects of obesity, alcohol and serum lipids on risk. Epidemiological and biomarker data from a UK prospective cohort study (EPIC-Norfolk). *Eur. J. Gastroenterol. Hepatol.* **23:** 733–740.
3. Malik, V. S., W. C. Willett, and F. B. Hu. 2013. Global obesity: trends, risk factors and policy implications. *Nat. Rev. Endocrinol.* **9:** 13–27.
4. World Health Organization. 2009. Global Health Risks: Mortality and Burden of Disease Attributable to Selected Major Risks. World Health Organization, Geneva.
5. Blecker, S., R. Herbert, and F. L. Brancati. 2012. Comorbid diabetes and end-of-life expenditures among Medicare beneficiaries with heart failure. *J. Card. Fail.* **18:** 41–46.
6. Hill, A. A., W. Reid Bolus, and A. H. Hasty. 2014. A decade of progress in adipose tissue macrophage biology. *Immunol. Rev.* **262:** 134–152.
7. Lumeng, C. N., and A. R. Saltiel. 2011. Inflammatory links between obesity and metabolic disease. *J. Clin. Invest.* **121:** 2111–2117.
8. Doyle, A. G., G. Herbein, L. J. Montaner, A. J. Minty, D. Caput, P. Ferrara, and S. Gordon. 1994. Interleukin-13 alters the activation state of murine macrophages in vitro: comparison with interleukin-4 and interferon-gamma. *Eur. J. Immunol.* **24:** 1441–1445.
9. Mantovani, A., A. Sica, and M. Locati. 2005. Macrophage polarization comes of age. *Immunity.* **23:** 344–346.
10. Martinez, F. O., A. Sica, A. Mantovani, and M. Locati. 2008. Macrophage activation and polarization. Front. *B*iosci. 13**:** 453–461.
11. Fujisaka, S., I. Usui, A. Bukhari, M. Ikutani, T. Oya, Y. Kanatani, K. Tsuneyama, Y. Nagai, K. Takatsu, M. Urakaze, et al. 2009. Regulatory mechanisms for adipose tissue M1 and M2 macrophages in diet-induced obese mice. *Diabetes.* **58:** 2574–2582.
12. Wentworth, J. M., G. Naselli, W. A. Brown, L. Doyle, B. Phipson, G. K. Smyth, M. Wabitsch, P. E. O'Brien, and L. C. Harrison. 2010. Pro-inflammatory CD11c+CD206+ adipose tissue macrophages are associated with insulin resistance in human obesity. *Diabetes.* **59:** 1648–1656.
13. Aron-Wisnewsky, J., J. Tordjman, C. Poitou, F. Darakhshan, D. Hugol, A. Basdevant, A. Aissat, M. Guerre-Millo, and K. Clement. 2009. Human adipose tissue macrophages: M1 and M2 cell surface markers in subcutaneous and omental depots and after weight loss. *J. Clin. Endocrinol. Metab.* **94:** 4619–4623.
14. Cinti, S., G. Mitchell, G. Barbatelli, I. Murano, E. Ceresi, E. Faloia, S. Wang, M. Fortier, A. S. Greenberg, and M. S. Obin. 2005. Adipocyte death defines macrophage localization and function in adipose tissue of obese mice and humans. *J. Lipid Res.* **46:** 2347–2355.
15. Kosteli, A., E. Sugaru, G. Haemmerle, J. F. Martin, J. Lei, R. Zechner, and A. W. Ferrante, Jr. 2010. Weight loss and lipolysis promote a dynamic immune response in murine adipose tissue. *J. Clin. Invest.* **120:** 3466–3479.
16. Shapiro, H., T. Pecht, R. Shaco-Levy, I. Harman-Boehm, B. Kirshtein, Y. Kuperman, A. Chen, M. Bluher, I. Shai, and A. Rudich. 2013. Adipose tissue foam cells are present in human obesity. *J. Clin. Endocrinol. Metab.* **98:** 1173–1181.
17. Edgel, K. A., T. S. McMillen, H. Wei, N. Pamir, B. A. Houston, M. T. Caldwell, P. O. Mai, J. F. Oram, C. Tang, and R. C. Leboeuf. 2012. Obesity and weight loss result in increased adipose tissue ABCG1 expression in db/db mice. *Biochim. Biophys. Acta.* **1821:** 425–434.
18. Angel, A., and B. Fong. 1983. Lipoprotein interactions and cholesterol metabolism in human fat cells. *In* The Adipocyte and Obesity: Cellular and Molecular Mechanisms. A. Angel, C. H. Hollenberg, and D. A. K. Roncari, editors. Raven, New York. 179–190.
19. Farkas, J., A. Angel, and M. I. Avigan. 1973. Studies on the compartmentation of lipid in adipose cells. II. Cholesterol accumulation and distribution in adipose tissue components. *J. Lipid Res.* **14:** 344–356.
20. Schreibman, P. H., and R. B. Dell. 1975. Human adipocyte cholesterol. Concentration, localization, synthesis, and turnover. *J. Clin. Invest.* **55:** 986–993.
21. Krause, B. R., and A. D. Hartman. 1984. Adipose tissue and cholesterol metabolism. *J. Lipid Res.* **25:** 97–110.
22. Arner, P. 1997. Is familial combined hyperlipidaemia a genetic disorder of adipose tissue? *Curr. Opin. Lipidol.* **8:** 89–94.
23. Zhao, S. P., Z. H. Wu, S. C. Hong, H. J. Ye, and J. Wu. 2006. Effect of atorvastatin on SR-BI expression and HDL-induced cholesterol efflux in adipocytes of hypercholesterolemic rabbits. *Clin. Chim. Acta.* **365:** 119–124.
24. Blanchette-Mackie, E. J., N. K. Dwyer, T. Barber, R. A. Coxey, T. Takeda, C. M. Rondinone, J. L. Theodorakis, A. S. Greenberg, and C. Londos. 1995. Perilipin is located on the surface layer of intracellular lipid droplets in adipocytes. *J. Lipid Res.* **36:** 1211–1226.
25. Ducharme, N. A., and P. E. Bickel. 2008. Lipid droplets in lipogenesis and lipolysis. *Endocrinology.* **149:** 942–949.
26. Arner, P. 2005. Human fat cell lipolysis: biochemistry, regulation and clinical role. *Best Pract. Res. Clin. Endocrinol. Metab.* **19:** 471–482.
27. Le Lay, S., P. Ferre, and I. Dugail. 2004. Adipocyte cholesterol balance in obesity. *Biochem. Soc. Trans.* **32:** 103–106.
28. Le Lay, S., C. Robichon, X. Le Liepvre, G. Dagher, P. Ferre, and I. Dugail. 2003. Regulation of ABCA1 expression and cholesterol efflux during adipose differentiation of 3T3–L1 cells. *J. Lipid Res.* **44:** 1499–1507.
29. Zhang, Y., F. C. McGillicuddy, C. C. Hinkle, S. O'Neill, J. M. Glick, G. H. Rothblat, and M. P. Reilly. 2010. Adipocyte modulation of high-density lipoprotein cholesterol. *Circulation.* **121:** 1347–1355.
30. Johansson, L. E., A. P. Danielsson, H. Parikh, M. Klintenberg, F. Norstrom, L. Groop, and M. Ridderstrale. 2012. Differential gene expression in adipose tissue from obese human subjects during weight loss and weight maintenance. *Am. J. Clin. Nutr.* **96:** 196–207.
31. Tarling, E. J. 2013. Expanding roles of ABCG1 and sterol transport. *Curr. Opin. Lipidol.* **24:** 138–146.
32. Tarling, E. J., and P. A. Edwards. 2011. ATP binding cassette transporter G1 (ABCG1) is an intracellular sterol transporter. *Proc. Natl. Acad. Sci. USA.* **108:** 19719–19724.
33. Sturek, J. M., J. D. Castle, A. P. Trace, L. C. Page, A. M. Castle, C. Evans-Molina, J. S. Parks, R. G. Mirmira, and C. C. Hedrick. 2010. An intracellular role for ABCG1-mediated cholesterol transport in the regulated secretory pathway of mouse pancreatic beta cells. *J. Clin. Invest.* **120:** 2575–2589.
34. Kennedy, M. A., A. Venkateswaran, P. T. Tarr, I. Xenarios, J. Kudoh, N. Shimizu, and P. A. Edwards. 2001. Characterization of the human ABCG1 gene: liver X receptor activates an internal promoter that produces a novel transcript encoding an alternative form of the protein. *J. Biol. Chem.* **276:** 39438–39447.
35. O'Connell, B. J., M. Denis, and J. Genest. 2004. Cellular physiology of cholesterol efflux in vascular endothelial cells. *Circulation.* **110:** 2881–2888.
36. Lorkowski, S., M. Kratz, C. Wenner, R. Schmidt, B. Weitkamp, M. Fobker, J. Reinhardt, J. Rauterberg, E. A. Galinski, and P. Cullen. 2001. Expression of the ATP-binding cassette transporter gene ABCG1 (ABC8) in Tangier disease. *Biochem. Biophys. Res. Commun.* **283:** 821–830.
37. Clunn, G. F., J. S. Refson, J. S. Lymn, and A. D. Hughes. 1997. Platelet-derived growth factor beta-receptors can both promote and inhibit chemotaxis in human vascular smooth muscle cells. *Arterioscler. Thromb. Vasc. Biol.* **17:** 2622–2629.
38. Malur, A., I. Huizar, G. Wells, B. P. Barna, A. G. Malur, and M. J. Thomassen. 2011. Lentivirus-ABCG1 instillation reduces lipid accumulation and improves lung compliance in GM-CSF knock-out mice. *Biochem. Biophys. Res. Commun.* **415:** 288–293.
39. Paschos, P., and K. Paletas. 2009. Non alcoholic fatty liver disease and metabolic syndrome. *Hippokratia.* **13:** 9–19.
40. Stokes, C. S., L. L. Gluud, M. Casper, and F. Lammert. 2014. Ursodeoxycholic acid and diets higher in fat prevent gallbladder

stones during weight loss: a meta-analysis of randomized controlled trials. Clin. *G*astroenterol. *H*epatol. 12**:** 1090–1100.e2; quiz e61.
41. Kennedy, M. A., G. C. Barrera, K. Nakamura, A. Baldan, P. Tarr, M. C. Fishbein, J. Frank, O. L. Francone, and P. A. Edwards. 2005. ABCG1 has a critical role in mediating cholesterol efflux to HDL and preventing cellular lipid accumulation. *Cell Metab.* **1:** 121–131.
42. McMillen, T. S., J. W. Heinecke, and R. C. LeBoeuf. 2005. Expression of human myeloperoxidase by macrophages promotes atherosclerosis in mice. *Circulation.* **111:** 2798–2804.
43. Pamir, N., T. S. McMillen, Y. I. Li, C. M. Lai, H. Wong, and R. C. LeBoeuf. 2009. Overexpression of apolipoprotein A5 in mice is not protective against body weight gain and aberrant glucose homeostasis. *Metabolism.* **58:** 560–567.
44. Taicher, G. Z., F. C. Tinsley, A. Reiderman, and M. L. Heiman. 2003. Quantitative magnetic resonance (QMR) method for bone and whole-body-composition analysis. *Anal. Bioanal. Chem.* **377:** 990–1002.
45. Tinsley, F. C., G. Z. Taicher, and M. L. Heiman. 2004. Evaluation of a quantitative magnetic resonance method for mouse whole body composition analysis. *Obes. Res.* **12:** 150–160.
46. Pamir, N., T. S. McMillen, K. J. Kaiyala, M. W. Schwartz, and R. C. LeBoeuf. 2009. Receptors for tumor necrosis factor-alpha play a protective role against obesity and alter adipose tissue macrophage status. *Endocrinology.* **150:** 4124–4134.
47. Honda, A., K. Yamashita, T. Hara, T. Ikegami, T. Miyazaki, M. Shirai, G. Xu, M. Numazawa, and Y. Matsuzaki. 2009. Highly sensitive quantification of key regulatory oxysterols in biological samples by LC-ESI-MS/MS. *J. Lipid Res.* **50:** 350–357.
48. Gersuk, G., A. Hiraoka, and K. A. Marr. 2005. Human monocytes differentiate into macrophages under the influence of human KPB-M15 conditioned medium. *J. Immunol. Methods.* **299:** 99–106.
49. Frevert, C. W., V. A. Wong, R. B. Goodman, R. Goodwin, and T. R. Martin. 1998. Rapid fluorescence-based measurement of neutrophil migration in vitro. *J. Immunol. Methods.* **213:** 41–52.
50. Nestor Kalinoski, A. L., R. S. Ramdath, K. M. Langenderfer, S. Sikanderkhel, S. Deraedt, M. Welch, J. L. Park, T. Pringle, B. Joe, G. T. Cicila, et al. 2010. Neointimal hyperplasia and vasoreactivity are controlled by genetic elements on rat chromosome 3. *Hypertension.* **55:** 555–561.
51. Wei, H., M. M. Averill, T. S. McMillen, F. Dastvan, P. Mitra, S. Subramanian, C. Tang, A. Chait, and R. C. Leboeuf. 2014. Modulation of adipose tissue lipolysis and body weight by high-density lipoproteins in mice. *Nutr. Diabetes.* **4:** e108.
52. Vaughan, A. M., and J. F. Oram. 2005. ABCG1 redistributes cell cholesterol to domains removable by high density lipoprotein but not by lipid-depleted apolipoproteins. *J. Biol. Chem.* **280:** 30150–30157.
53. Wang, N., D. Lan, W. Chen, F. Matsuura, and A. R. Tall. 2004. ATP-binding cassette transporters G1 and G4 mediate cellular cholesterol efflux to high-density lipoproteins. *Proc. Natl. Acad. Sci. USA.* **101:** 9774–9779.
54. Olivier, M., M. W. Tanck, R. Out, E. F. Villard, B. Lammers, L. Bouchareychas, E. Frisdal, A. Superville, T. Van Berkel, J. J. Kastelein, et al. 2012. Human ATP-binding cassette G1 controls macrophage lipoprotein lipase bioavailability and promotes foam cell formation. *Arterioscler. Thromb. Vasc. Biol.* **32:** 2223–2231.
55. Whetzel, A. M., J. M. Sturek, M. H. Nagelin, D. T. Bolick, A. K. Gebre, J. S. Parks, A. C. Bruce, M. D. Skaflen, and C. C. Hedrick. 2010. ABCG1 deficiency in mice promotes endothelial activation and monocyte-endothelial interactions. *Arterioscler. Thromb. Vasc. Biol.* **30:** 809–817.
56. Baldan, A., A. Gonen, C. Choung, X. Que, T. J. Marquart, I. Hernandez, I. Bjorkhem, D. A. Ford, J. L. Witztum, and E. J. Tarling. 2014. ABCG1 is required for pulmonary B-1 B cell and natural antibody homeostasis. *J. Immunol.* **193:** 5637–5648.
57. Pagler, T. A., M. Wang, M. Mondal, A. J. Murphy, M. Westerterp, K. J. Moore, F. R. Maxfield, and A. R. Tall. 2011. Deletion of ABCA1 and ABCG1 impairs macrophage migration because of increased Rac1 signaling. *Circ. Res.* **108:** 194–200.
58. Lumeng, C. N., J. L. Bodzin, and A. R. Saltiel. 2007. Obesity induces a phenotypic switch in adipose tissue macrophage polarization. *J. Clin. Invest.* **117:** 175–184.
59. Venkateswaran, A., B. A. Laffitte, S. B. Joseph, P. A. Mak, D. C. Wilpitz, P. A. Edwards, and P. Tontonoz. 2000. Control of cellular cholesterol efflux by the nuclear oxysterol receptor LXR alpha. *Proc. Natl. Acad. Sci. USA.* **97:** 12097–12102.
60. Wójcicka, G., A. Jamroz-Wiśniewska, K. Horoszewicz, and J. Beltowski. 2007. Liver X receptors (LXRs). Part I: structure, function, regulation of activity, and role in lipid metabolism. *Postepy Hig. Med. Dosw. (Online).* **61:** 736–759.
61. Kratz, M., B. R. Coats, K. B. Hisert, D. Hagman, V. Mutskov, E. Peris, K. Q. Schoenfelt, J. N. Kuzma, I. Larson, P. S. Billing, et al. 2014. Metabolic dysfunction drives a mechanistically distinct proinflammatory phenotype in adipose tissue macrophages. *Cell Metab.* **20:** 614–625.
62. Ghosn, E. E., A. A. Cassado, G. R. Govoni, T. Fukuhara, Y. Yang, D. M. Monack, K. R. Bortoluci, S. R. Almeida, L. A. Herzenberg, and L. A. Herzenberg. 2010. Two physically, functionally, and developmentally distinct peritoneal macrophage subsets. *Proc. Natl. Acad. Sci. USA.* **107:** 2568–2573.
63. Selvarajan, K., L. Moldovan, A. N. Chandrakala, D. Litvinov, and S. Parthasarathy. 2011. Peritoneal macrophages are distinct from monocytes and adherent macrophages. *Atherosclerosis.* **219:** 475–483.
64. Buchmann, J., C. Meyer, S. Neschen, R. Augustin, K. Schmolz, R. Kluge, H. Al-Hasani, H. Jurgens, K. Eulenberg, R. Wehr, et al. 2007. Ablation of the cholesterol transporter adenosine triphosphate-binding cassette transporter G1 reduces adipose cell size and protects against diet-induced obesity. *Endocrinology.* **148:** 1561–1573.
65. Gordon, S. 2003. Alternative activation of macrophages. *Nat. Rev. Immunol.* **3:** 23–35.
66. Hume, D. A. 2015. The many alternative faces of macrophage activation. *Front. Immunol.* **6:** 370.
67. Tabas, I. 2010. Macrophage death and defective inflammation resolution in atherosclerosis. *Nat. Rev. Immunol.* **10:** 36–46.
68. Burgess, B. L., P. F. Parkinson, M. M. Racke, V. Hirsch-Reinshagen, J. Fan, C. Wong, S. Stukas, L. Theroux, J. Y. Chan, J. Donkin, et al. 2008. ABCG1 influences the brain cholesterol biosynthetic pathway but does not affect amyloid precursor protein or apolipoprotein E metabolism in vivo. *J. Lipid Res.* **49:** 1254–1267.
69. Vallières, L., and P. E. Sawchenko. 2003. Bone marrow-derived cells that populate the adult mouse brain preserve their hematopoietic identity. *J. Neurosci.* **23:** 5197–5207.
70. Liddle, R. A., R. B. Goldstein, and J. Saxton. 1989. Gallstone formation during weight-reduction dieting. *Arch. Intern. Med.* **149:** 1750–1753.